

Magnetic oscillations in a two-dimensional network of compensated electron and hole orbits

A. AUDOUARD¹(*), D. VIGNOLLES¹, E. HAANAPPEL¹, I. SHEIKIN², R. B. LYUBOVSKIĬ³
AND R. N. LYUBOVSKAYA³

¹ *Laboratoire National des Champs Magnétiques Pulsés (UMR CNRS-UPS-INSA 5147),
143 avenue de Rangueil, 31432 Toulouse cedex 4, France*

² *Grenoble High Magnetic Field Laboratory, CNRS, BP166, 38042 Grenoble Cedex 9,
France*

³ *Institute of Problems of Chemical Physics, Russian Academy of Sciences, Chernogolovka,
Moscow oblast, 142432 Russia*

PACS. 71.18.+y – Fermi surface: calculations and measurements; effective mass, g factor.

PACS. 72.15.Gd – Galvanomagnetic and other magnetotransport effects.

PACS. 71.20.Rv – Polymers and organic compounds.

Abstract. – The Fermi surface of the quasi-two dimensional (2D) organic metal (ET)₈Hg₄Cl₁₂ (C₆H₅Br)₂ can be regarded as a 2D network of compensated electron and hole orbits coupled by magnetic breakthrough. Simultaneous measurements of the interlayer magnetoresistance and magnetic torque have been performed for various directions of the magnetic field up to 28 T in the temperature range from 0.36 K to 4.2 K. Magnetoresistance and de Haas-van Alphen (dHvA) oscillations spectra exhibit frequency combinations typical of such a network. Even though some of the observed magnetoresistance oscillations cannot be interpreted on the basis of neither conventional Shubnikov-de Haas oscillations nor quantum interference, the temperature and magnetic field (both orientation and magnitude) dependence of all the Fourier components of the dHvA spectra can be consistently accounted for by the dHvA effect on the basis of the Lifshitz-Kosevich formula. This behaviour is at variance with that currently reported for compounds illustrating the linear chain of coupled orbits model.

Frequency combinations observed in magnetic oscillations spectra of multiband quasi two-dimensional (2D) metals have been extensively studied both from theoretical and experimental viewpoints [1]. Nevertheless, the physical origin of some of the observed Fourier components, the so called 'forbidden frequencies', remain still unclear. In addition to quantum interference (QI) that can be invoked in the case of magnetoresistance (MR) data, these frequencies can be attributed to both the oscillation of the chemical potential [2,3] and the field-dependent magnetic breakthrough (MB)-induced Landau level broadening [4]. However, a quantitative model that involve these two latter contributions is still needed. The Fermi surface (FS) of most of the compounds exhibiting such frequencies corresponds to the linear chain of coupled orbits model. This model was introduced by Pippard in the early sixties in order to compute

(*) E-mail: audouard@lncmp.org

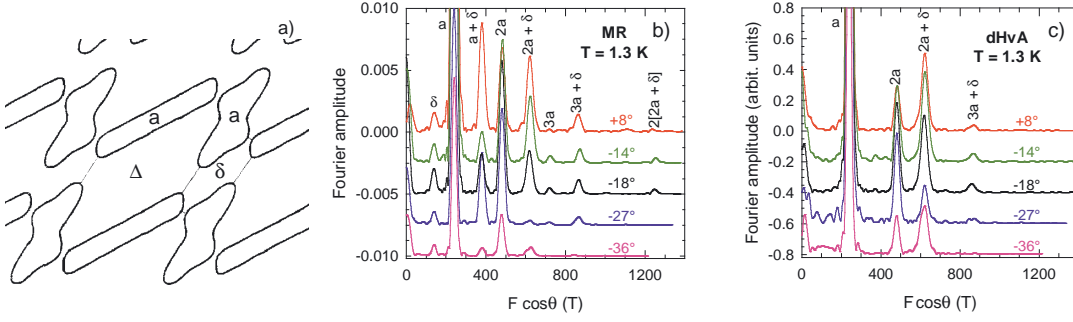


Fig. 1 – (a) Fermi surface of $(\text{ET})_8\text{Hg}_4\text{Cl}_{12}(\text{C}_6\text{H}_5\text{Cl})_2$ according to band structure calculations of Veiros et al. [6]. In addition to the compensated elongated electron and hole closed orbits a , the δ and Δ pieces are indicated. Fourier analysis of (b) magnetoresistance and (c) de Haas-van Alphen oscillations for various directions of the magnetic field at 1.3 K.

MB-induced de Haas-van Alphen (dHvA) oscillation spectrum in a one-dimensional network of electronic orbits [5]. More recently, the 2D network of compensated electron and hole orbits without any non-quantized electron reservoir, realized by the FS of the isostructural organic metals $(\text{ET})_8\text{Hg}_4\text{Cl}_{12}(\text{C}_6\text{H}_5\text{X})_2$ where ET stands for bis(ethylenedithio)tetrathiafulvalene and $\text{X} = \text{Cl}, \text{Br}$ (see Fig. 1a and Ref. [6]), has been considered [7–9]. Contrary to the β -(ET)₂I Br_2 salt whose oscillatory spectra exhibit either additional slow oscillations or beatings due to a significantly warped FS [10], the above compounds are strongly 2D [7]. The MB orbits and QI paths liable to be involved in the oscillatory spectra are described in Refs. [8, 9]. The Fourier spectra of the oscillatory MR have been analyzed on the basis of the Falicov and Stachowiak model [11] which assumes that the effective mass of a given MB orbit is the sum of the effective masses of each of its components. In agreement with this model, the effective mass of, e. g., the MB-induced $2a + \delta$ orbit observed in MR experiments is about twice that of the compensated ‘basic’ orbits a . In addition to these Shubnikov-de Haas (SdH) orbits, some of the observed Fourier components could be attributed to QI linked to e. g. $a + \delta$ and $b = 2a + \delta + \Delta$ interferometers. Nevertheless, in view of the measured values of the MB field and of the relevant effective masses, the field dependence of the oscillation amplitude of $a + \delta$ is not in agreement with such a picture. Moreover, other components such as δ which has a very low effective mass (see Table I) cannot be understood on the basis of neither SdH orbits nor QI. Previous attempts at measuring the oscillatory magnetization which, as a thermodynamic parameter, should be insensitive to QI, revealed that the effective mass linked to SdH and dHvA oscillations of the closed orbits a and $2a + \delta$, respectively, is the same within the error bars [9, 12]. However, the signal-to-noise ratio was too weak in order to obtain reliable results for other Fourier components.

In this letter, we present simultaneous measurements of MR and dHvA oscillations of $(\text{ET})_8\text{Hg}_4\text{Cl}_{12}(\text{C}_6\text{H}_5\text{Br})_2$ for various directions of the magnetic field up to 28 T. Even though ‘forbidden frequencies’ are evidenced in MR oscillations spectra, it is demonstrated that, at variance with compounds whose FS illustrates the linear chain model, the behaviour of the frequency combinations observed in dHvA spectra of this network of compensated orbits can be consistently accounted for by the Falicov and Stachowiak model on the basis of the Lifshits-Kosevich (LK) formula.

The studied crystal is a platelet with approximate dimensions $(1 \times 1 \times 0.1) \text{ mm}^3$, the largest sides being parallel to the conducting bc -plane. MR and magnetic torque measurements were

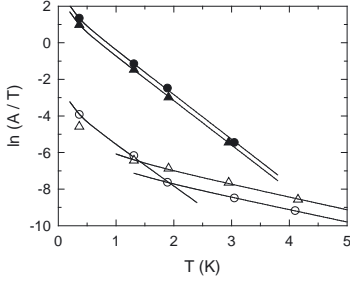


Fig. 2

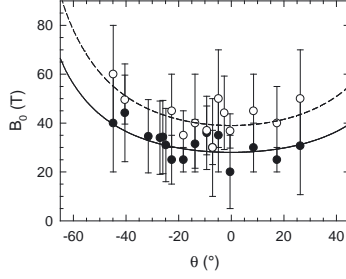


Fig. 3

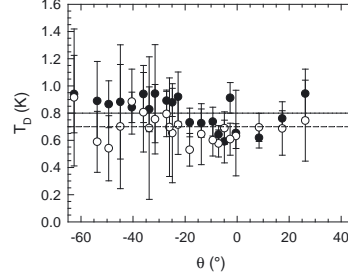


Fig. 4

Fig. 2 – Temperature dependence of the Fourier amplitude (A) of magnetoresistance (MR, open symbols) and de Haas-van Alphen (dHvA, solid symbols) data for the $3a + \delta$ component at a mean value of the magnetic field $\bar{B} = 21.4$ T. The angle between the field direction and the normal to the conducting plane is 17° and -27° , for circles and triangles, respectively. Solid lines are best fits of Eqs. 1 and 2 to MR and dHvA data, respectively.

Fig. 3 – Mean magnetic breakdown field values (B_0) deduced from the field dependence of the amplitude of the a oscillations at 1.3 K for various field directions. Closed and open symbols stand for dHvA and Shubnikov-de Haas (SdH) data, respectively. Solid and dashed line are best fits to the dHvA and SdH data, respectively, assuming an orbital behaviour.

Fig. 4 – Same as Fig. 3 for the Dingle temperature. Solid and dashed line corresponds to the mean value of dHvA ($T_D = 0.8$ K) and SdH ($T_D = 0.7$ K) data, respectively.

performed simultaneously up to 28 T at the M10 resistive magnet of the Grenoble High Magnetic Field Laboratory. A one axis rotating sample holder allowed to change the direction of the magnetic field with respect to the conducting plane. In the following, θ is the angle between the magnetic field direction and the a^* axis. Experiments were performed in the temperature range from 0.36 K to 4.2 K for $\theta = -27^\circ, -18^\circ, 8^\circ$ and 17° and at 1.3 K for $-62^\circ \leq \theta \leq 26^\circ$ (the sign of θ is arbitrary). Electrical contacts were made to the crystal for MR measurements using annealed gold wires of 10 μm in diameter glued with graphite paste. Alternating current (10 μA , 10 Hz) was injected parallel to the a^* direction (interlayer configuration). A lock-in amplifier was used to detect the signal across the potential leads. Magnetic torque was measured by the cantilever method [13]. Its oscillatory part is given by $\tau = -(1/F)M_{\parallel}(\partial F/\partial \theta)BV$ [13–15] where M_{\parallel} is the component of the oscillatory magnetization parallel to B and V is the crystal volume. For a 2D FS, the oscillation frequency varies as $F = F(\theta = 0)/\cos(\theta)$ and τ is therefore proportional to $M_{\parallel}/B \tan \theta$.

In the framework of the 2D LK model, the measured Fourier amplitudes (A_i) of the various components of the normalized oscillatory MR ($R_{osc}/R_{bg} - 1$, where R_{osc} and R_{bg} is the oscillatory and background resistance, respectively) and of the torque are respectively given by [14]:

$$A_i(MR) \propto R_{Ti} R_{Di} R_{MBi} R_{Si} \quad (1)$$

and

$$A_i(\text{torque}) \propto B R_{Ti} R_{Di} R_{MBi} R_{Si} \tan \theta, \quad (2)$$

For a 2D FS, the measured effective mass (expressed in m_e units in the following) depends on the field direction as $m_i^* = m_i^*(\theta = 0)/\cos(\theta)$. This angle dependence has been checked in Refs. [9, 12] for the presently studied compound. The thermal and Dingle damping factors are therefore respectively given by $R_{Ti} = \alpha T m_i^*(\theta = 0)/B \cos(\theta) \sinh[\alpha T m_i^*(\theta = 0)/B \cos(\theta)]$ and

TABLE I – Effective mass [$m^*(\theta = 0)$] and μ parameter ($\mu = g^* m_i^*(\theta = 0)/2$) deduced from temperature and field direction dependence, respectively, of the Fourier components indicated in the left column.

	$m^*(\theta = 0)$				μ	
	MR [9]	dHvA [12]	MR	dHvA	MR	dHvA
δ	0.45±0.10		0.3±0.1			
a	1.17±0.13	1.15±0.12	1.23±0.04	1.23±0.04	1.28±0.04	1.25±0.03
$a + \delta$	1.00±0.07		1.06±0.07			
$2a + \delta$	2.10±0.16	2.10±0.25	2.15±0.15	2.15±0.13	2.2±0.1	2.15±0.15
$3a + \delta$ (high T)	0.72±0.06		0.9±0.1	3.1±0.3		2.75±0.20
$3a + \delta$ (low T)	2.95±0.20		3.1±0.3			

$R_{Di} = \exp[-\alpha T_D m_i^*(\theta = 0)/B \cos(\theta)]$, where $\alpha = 2\pi^2 k_B m_e / e\hbar$ ($\simeq 14.69$ T/K) and T_D is the Dingle temperature. The spin and MB damping factors are given by:

$$R_{Si} = |\cos(\pi\mu / \cos\theta)| \quad (3)$$

and

$$R_{MBi} = \prod_{g=1,2} p_g^{t_g} q_g^{b_g}, \quad (4)$$

respectively, where $\mu = g^* m_i^*(\theta = 0)/2$ and g^* is the effective Landé factor. The index g stands for the 2 different gaps between electron and hole orbits (see Fig. 1a and Ref. [9]). Integers t_g and b_g are respectively the number of tunnelling and Bragg reflections encountered along the path of the quasiparticle. The tunnel and Bragg reflection probability amplitudes are given by $p_g^2 = \exp(-B_g/B)$, where B_g is the MB field, and $p_g^2 + q_g^2 = 1$. As discussed in Ref. [9], only a mean value B_0 of the two MB fields can be derived from experimental data. Eq. 4 then reduces to $R_{MBi} = p^t q^b$ where $p^2 = \exp(-B_0/B)$. Calculations of R_{MBi} and effective masses for various orbits are given in Ref. [9].

In addition to the frequency linked to the 'basic' orbits a , Fourier analysis of the MR oscillations reveals combinations frequencies involving the δ piece of the FS, in good agreement with data from Ref. [9] (see Fig. 1b). Nevertheless, since the maximum field reached in the experiments is lower than in Ref. [9], the high frequency components, in particular those involving the Δ piece of the FS cannot be observed. As it is the case for MR data, dHvA spectra also present frequency combinations. Nevertheless, δ and $a + \delta$ components are clearly absent in Fig. 1c. Except for few MR components at high field, as developed later on, the temperature dependence of the observed oscillations is satisfactorily accounted for by the LK formalism. The deduced values of the effective masses are reported in Table I. A good agreement between MR and dHvA data is observed for a and $2a + \delta$ closed orbits. Oppositely, the behaviour of the $3a + \delta$ component calls for some comments. Indeed, a change of the effective mass deduced from MR data has been reported in Ref. [9], in agreement with data in Fig. 2. Generally speaking, the effective mass deduced from low temperature data is in agreement with a MB-induced orbit while the high temperature value, which is about 3 times lower, is consistent with QI. In contrast, no change of the effective mass is observed in dHvA data which otherwise are in agreement with a MB-induced orbit. In summary, at variance with MR data, the effective mass values deduced from all the Fourier components of the torque data can be interpreted, in the framework of the Falicov and Stachowiak model, on the basis of dHvA effect linked to, eventually MB-induced, closed orbits.

This can further be checked by considering the field dependence of the Fourier components. A quantitative analysis of these data requires first the determination of the MB field

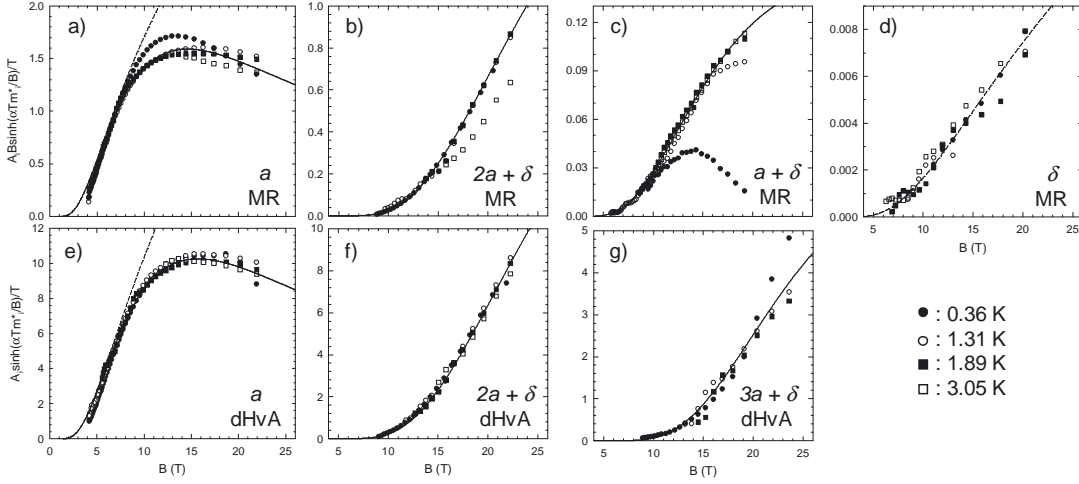


Fig. 5 – Magnetic field dependence, for $\theta = 17^\circ$, of the Fourier amplitude of (a) to (d) magnetoresistance (MR) and (e) to (g) de Haas-van Alphen (dHvA) components normalized by the relevant thermal damping factor R_{Ti} for $i = \delta, a, a + \delta, 2a + \delta$ and $3a + \delta$. Solid lines are best fits of Eqs. 1 and 2 to MR and dHvA data, respectively, with $B_0 = 25$ T. Dashed lines are obtained with $R_{MBi} = 1$. The Dingle temperature is in the range 0.6 K to 0.7 K, except for δ which cannot be accounted for by a closed orbit and $a + \delta$ for which the solid line corresponds to a negative value.

B_0 . Since the a orbit only involves Bragg reflections, the most pronounced damping of the oscillation amplitude as the magnetic field increases is observed for this component. This feature allows us to determine B_0 , as well as T_D , from the field dependence of the amplitude of this oscillation series. The angle dependence of the MB field deduced from the analysis of the data collected at 1.3 K in the range $-62^\circ \leq \theta \leq 26^\circ$ is compatible with an orbital behaviour and yields $B_0(\theta = 0) = (28 \pm 9)$ T and (39 ± 10) T, for dHvA and SdH oscillations, respectively (see Fig. 3). Besides, the Dingle temperature reported in Fig. 4 can be regarded as temperature-independent: $T_D = (0.8 \pm 0.2)$ K and $T_D = (0.7 \pm 0.2)$ K for dHvA and SdH data, respectively. According to the LK formula, the temperature-independent part of the amplitude is given by A_i/R_{Ti} . As an example, data for $\theta = 17^\circ$ are given in Fig. 5. In agreement with the LK model, all the dHvA data related to the a component lie on the same curve (see Fig. 5e) and are accounted for by $B_0 = 25$ T and $T_D = 0.7$ K. The same value of effective mass as for dHvA data is used for the analysis of MR data in Fig. 5a. Data at low field yield $T_D = 0.6$ K which is in good agreement with data of Fig. 4 and with dHvA data of Fig. 5e. However, some discrepancies can be observed at fields higher than a few teslas, in particular at the lowest temperature. This feature puts some doubts on the value of B_0 extracted from MR data, which otherwise is in good agreement with data from Ref. [9] [$B_0 = (35 \pm 7)$ T]. Regarding the MB-induced $2a + \delta$ orbit, both MR and dHvA data are consistent with each other and with the data for the a component. Namely, assuming $B_0 = 25$ T, the solid line in Figs. 5b and f correspond to $T_D = 0.7$ K, in good agreement with data for the a oscillations. Analogous result is obtained for dHvA data related to the $3a + \delta$ component ($T_D = 0.7$ K, see Fig. 5g). Oppositely, the $a + \delta$ component observed in MR, which has been attributed to QI, exhibits significant discrepancies with the LK formalism at low temperature and high field (see Fig. 5c). In addition, the Dingle temperature value deduced from the solid line in the figure is negative ($T_D = -0.5$ K), as it is the case for the data reported in Ref. [9].

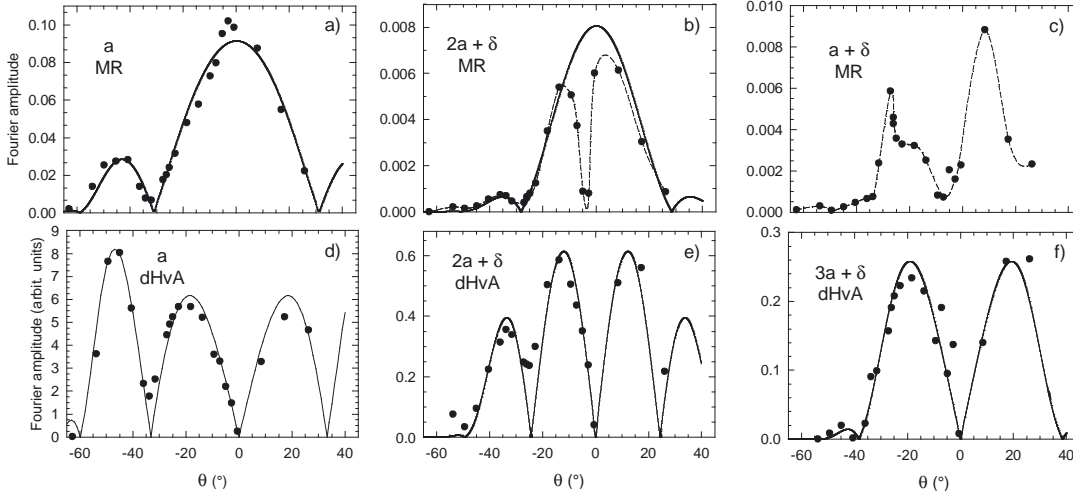


Fig. 6 – Angle (θ) dependence of the (a, b, c) magnetoresistance (MR) and (d, e, f) de Haas-van Alphen (dHvA) Fourier amplitudes for a , $a + \delta$, $2a + \delta$ and $3a + \delta$ components at a temperature of 1.3 K and a mean value of the magnetic field $\bar{B} = 14.7$ T. Solid lines are best fits of Eqs. 1 and 2 to MR and dHvA data, respectively. Dashed lines are guides to the eye.

Finally, MR data for the δ component (see Fig. 5d) follow the LK behaviour even though this component cannot be interpreted on the basis of the Falicov and Stachowiak model. Recall that MR data for $3a + \delta$ cannot be considered due to the observed change of the effective mass as the temperature varies.

Lastly, let us consider the field direction dependence of the oscillations amplitude for which the spin damping factor (see Eq. 3) plays an important part. A good agreement with the LK model is observed for both MR and dHvA data related to the a oscillations (see Fig. 6). In addition, the deduced values of μ are very close to m^* (see Table I) which is in agreement with a Fermi liquid, as suggested in Ref. [16]. The same feature is observed for dHvA data of the $2a + \delta$ and $3a + \delta$ components. MR data for the MB orbit $2a + \delta$ evidence a strong damping at $\theta \approx -5^\circ$. Analogous damping of the MB orbit have also been observed, although at $\theta = 0^\circ$, in MR data of κ -(ET)₂I₃ [17, 18]. Some damping of the SdH oscillations linked to the 'basic' orbit of β'' -(ET)₂SF₅CH₂CF₂SO₃ is also reported in the high field and low temperature ranges [19]. This behaviour which is not observed for dHvA oscillations [17–19] has still not received a clear explanation. In spite of the damping observed in Fig. 6b, the data away from $\theta \approx -5^\circ$ is still in agreement with a μ value close to m^* . In contrast, the amplitude of the $a + \delta$ component, which is not symmetric with respect to θ , cannot be accounted for by the LK formula. As it is the case of $2a + \delta$, it exhibits a minima around $\theta \approx -5^\circ$.

In summary, all the observed torque components can be consistently interpreted on the basis of dHvA closed orbits. This is at variance with MR oscillations linked to (i) SdH closed orbits a and $2a + \delta$ which exhibit discrepancies at high field and at $\theta \approx -5^\circ$, respectively, and (ii) other components such as $a + \delta$ for which the field dependence is too weak in order to account for a positive T_D even though its effective mass is consistent with QI. Departures from the LK behaviour have already been reported for many clean crystals of quasi-2D organic metals. Therefore, the observed MR behaviour is not surprising. Regarding dHvA data, 'forbidden' frequency combinations with significant amplitude are observed in compounds illustrating the linear chain model. This is at variance with the presently observed

behaviour. As suggested in Ref. [20], this discrepancy could be due, for a part, to the nature of the considered orbits network for which the chemical potential might be pinned between electron and hole Landau levels. This problem, that actually remains to be solved, is of importance since the FS of many organic metals based on the ET molecule or one of its derivative constitutes a network of compensated electron and hole orbits as well.

* * *

We wish to acknowledge J. Y. Fortin and G. Rikken for interesting discussions. This work was supported by the CNRS-RAS cooperation agreement # 16390. RBL thanks RFBR 03-02-16606 for support.

REFERENCES

- [1] For a review, see e. g. KARTSOVNIK M., *Chem. Rev.*, **104** (2004) 5737 and references therein.
- [2] HARRISON N., CAULFIELD J., SINGLETON J., REINDERS P. H. P., HERLACH F., W. HAYES, M. KURMOO AND P. DAY, *J. Phys.: Condens. Matter*, **8** (1996) 5415.
- [3] KISHIGI K. AND HASEGAWA Y., *Phys. Rev. B*, **65** (2002) 205405.
- [4] SANDHU P. S., KIM J. H. AND BROOKS J. S., *Phys. Rev. B*, **56** (1997) 11566. FORTIN J. Y. AND ZIMAN T., *Phys. Rev. Lett.*, **80** (1998) 3117. KIM J. H., HAN S. Y. AND BROOKS J. S., *Phys. Rev. B*, **60** (1999) 3213. HAN S. Y., BROOKS J. S. AND KIM J. H., *Phys. Rev. Lett.*, **85** (2000) 1500. GVOZDIKOV V. M., PERSHIN YU V., STEEP E., JANSEN A. G. M. AND WYDER P., *Phys. Rev. B*, **65** (2002) 165102.
- [5] PIPPARD A. B., *Proc. Roy. Soc. (London)*, **A270** (1962) 1.
- [6] VIEROS L. F. AND CANADELL E., *J. Phys. (France) I*, **4** (1994) 939.
- [7] LYUBOVSKIĬ R. B., PESOTSKIĬ S. I., GILEVSKIĬ A. AND LYUBOVSKAYA R. N., *JETP*, **80** (1995) 1063 [*Zh. Éksp. Teor. Fiz.*, **107** (1995) 1698].
- [8] PROUST C., AUDOUARD A., BROSSARD L., PESOTSKIĬ S. I., LYUBOVSKIĬ R. B. AND LYUBOVSKAYA R. N., *Phys. Rev. B*, **65** (2002) 155106.
- [9] VIGNOLLES D., AUDOUARD A., BROSSARD L., PESOTSKIĬ S. I., B. LYUBOVSKIĬ R. AND LYUBOVSKAYA R. N., *Eur. Phys. J. B*, **31** (2003) 53.
- [10] M. V. KARTSOVNIK, P. D. GRIGORIEV, W. BIBERACHER, N. D. KUSHCH AND P. WYDER, *Phys. Rev. Lett.*, **89** (2002) 126802.
- [11] FALICOV L. M. AND STACHOWIAK H., *Phys. Rev.*, **147** (1966) 505.
- [12] AUDOUARD A., VIGNOLLES D., PROUST C., BROSSARD L., NARDONE M., HAANAPPEL E., PESOTSKIĬ S. I., B. LYUBOVSKIĬ R. AND LYUBOVSKAYA R. N., *Physica B*, **346-347** (2004) 377.
- [13] SHEIKIN I., GRÖGER A., RAYMOND S., JACCARD D., AOKI D., HARIMA H. AND FLOUQUET J., *Phys. Rev. B*, **67** (2003) 94420.
- [14] SHOENBERG D., *Magnetic Oscillations in Metals* (Cambridge Univ. Press, Cambridge) 1984.
- [15] WOSNITZA J., *Fermi Surfaces of Low-dimensional Organic Metals and Superconductors* (Springer-Verlag Berlin Heidelberg) 1996.
- [16] LYUBOVSKIĬ R. B., PESOTSKIĬ S. I., NIZHANKOVSKIĬ V. I., BIBERACHER W. AND LYUBOVSKAYA R. N., *JETP*, **98** (2004) 1037 [*Zh. Éksp. Teor. Fiz.*, **125** (2004) 1184].
- [17] BALTHES E., SCHWEITZER D., HEINEN I., STRUNZ W., BIBERACHER W., JANSEN A. G. M. AND STEEP E., *Z. Phys. B*, **99** (1996) 163.
- [18] HARRISON N., MIELKE C. N., RICKEL D. G., WOSNITZA J., QUALLS J. S., BROOKS J. S., BALTHES E., SCHWEITZER D., HEINEN I. AND STRUNZ W., *Phys. Rev. B*, **58** (1998) 10248.
- [19] WOSNITZA J., WANKA S., QUALLS J. S., MIELKE C. H., HARRISON N., SCHLUETER J. A., WILLIAMS J. M., NIXON P. G., WINTER R. W. AND GARD G. L., *Synth. Met.*, **103** (1999) 2000.
- [20] FORTIN J. Y., PEREZ E. AND AUDOUARD A., *Phys. Rev. B*, **71** (2005) 155101.